



## Theoretical DFT studies of chromium tricarbonyl complexes with polycyclic aromatic ligands

Yuri F. Oprunenko\*, Igor P. Glorizov

Department of Chemistry, M.V. Lomonosov Moscow State University, Vorob'evy Gory, 119899 Moscow, Russia

### ARTICLE INFO

#### Article history:

Received 23 August 2008  
Received in revised form 29 October 2008  
Accepted 14 November 2008  
Available online 14 December 2008

Dedicated to Professor Christoph Elschenbroich on the occasion of his 70th birthday.

#### Keywords:

Arenetricarbonylchromium complexes  
Polyaromatic carbo- and heterocyclic ligands  
Complex and ligand lithiation  
Interring haptotropic rearrangements  
Quantum chemical calculations  
Density functional theory

### ABSTRACT

This paper presents a theoretical analysis of the structures of tricarbonyl chromium complexes of carbo- and heterocyclic polyaromatic ligands (PAL) and the mechanisms of interring haptotropic rearrangement in such complexes performed by using density functional theory (DFT) with the nonempirically constructed PBE functional and extended split basis sets. The reaction paths were calculated for interring haptotropic rearrangements and rotations of the metallocarbonyl fragment in the regioisomeric complexes. The structures and energy characteristics of stationary points of the systems were determined. The migration of the  $\text{Cr}(\text{CO})_3$  group was shown to occur at the periphery of the ligand via transition states with the structure of  $\eta^3$ -allylic or  $\eta^4$ -trimethylmethane complexes. Calculated geometries of the complexes and the activation barriers were in a close agreement with the experimental data.

The reaction of  $\eta^6$ -tricarbonylchromium complexes of PAL with *n*-BuLi (*lithiation*) was also studied by the DFT. The *kinetic and thermodynamic factors* that control the direction and selectivity of metallation were calculated for the model  $\eta^6$ -biphenylenetricarbonylchromium complex. Both approaches indicate that lithiation occurs exclusively at the aromatic ring bonded to the transition metal, which agrees with the experimental data. The selectivity inside this ring is governed by a thermodynamic factor. The solvation effects were simulated for the lithium salt of the model  $\eta^6$ -naphthalenechromium tricarbonyl complex in which lithium is localized at the  $\alpha(1)$ -position of coordinated ring. The simulation showed the most stable coordination of the lithium atom with two THF molecules. Addition of extra THF molecules is thermodynamically unfavorable. The tricarbonylchromium complexes of naphthalene, biphenyl, biphenylene and dibenzothiophene calculated relative energies for all solvated by two THF molecules lithium salts indicate that the difference in energies  $\Delta E \leq 1$  kcal mol<sup>-1</sup> corresponds to the experimentally observed absence of selectivity, while the difference more than 2.5 kcal mol<sup>-1</sup> corresponds to the selectivity of the reaction. No additional coordination of lithium to heteroatom was observed for the sulfur-containing dibenzothiophene complex. Similar calculation shows that double metallation in the dibenzothiophene complex occurs at positions 1 and 4. The developed approach enables one to predict the direction and selectivity of metallation reactions of transition metal complexes with different arenes and thus to synthesize labeled complexes for the investigation of degenerate IRHR.

© 2008 Elsevier B.V. All rights reserved.

### 1. Introduction

Nowadays, tricarbonylchromium  $\pi$ -complexes with aromatic ligands are widely used in the organic and organometallic chemistry for both catalytic and synthetic purposes. These species are efficient precursors for the corresponding substituted complexes or organic aromatic derivatives due to their ability to provide fine regio- and stereochemical control of metallation reactions (e.g. *lithiation*) and subsequent reaction of the salt with the electrophile. Such reactions are used in the drug design. In particular, optically active principal components could be obtained due to the activat-

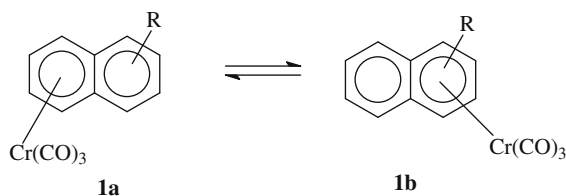
ing influence of the  $\text{Cr}(\text{CO})_3$  group with specific steric and electronic properties.

This important and large class of organometallic compounds was studied in most detail for carbocyclic monoaromatic ligands and, to a *less extent*, for polyaromatic ligands. All available data are comprehensively discussed in many reviews [1]. Such complexes, in which only a part of the ligand positions accessible for coordination is involved in bonding with a metal atom, are characterized by high lability. This is manifested in a variety of dynamic processes that take place in these compounds. Among these are intramolecular inter-ring haptotropic rearrangements (IRHR), which occur with migration of the metal atom from one position of the ligand to another [2].

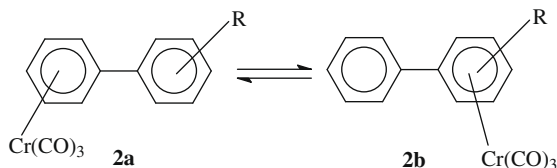
Previous attempts to prove the existence of degenerate IRHR ( $\eta^6, \eta^6$ -rearrangement from one ring to another) in transition

\* Corresponding author.

E-mail addresses: [oprunenko@nmr.chem.msu.su](mailto:oprunenko@nmr.chem.msu.su), [oprunenko@mail.ru](mailto:oprunenko@mail.ru) (Y.F. Oprunenko).



Scheme 1.



Scheme 2.

metal complexes of unsubstituted symmetric PAL by means of dynamic NMR without introducing a substituent-label into one of the six-membered rings of the ligand were unsuccessful due to usually *high value of activation barrier*. Thus, on heating  $^1\text{H}$  and  $^{13}\text{C}$  NMR spectra of the samples of  $\eta^6$ -acenaphthylene $\text{Cr}(\text{CO})_3$  [2],  $\eta^6$ - $\text{C}_{10}\text{H}_8\text{Cr}(\text{CO})_3$  [3],  $[(\eta^6\text{-C}_{10}\text{H}_8)\text{Ir}(\text{C}_5\text{Me}_5)]^{2-}(\text{PF}_6)_2$ , (70 °C,  $\text{CF}_3\text{COOH}$ ) [4],  $(\eta^6\text{-C}_{10}\text{H}_8)_2\text{Cr}$  (130 °C,  $\text{C}_6\text{D}_6$ ) [5] did not manifest the dynamic behavior on NMR time scale. Only recently fast intra- and interring rearrangements were found and thermodynamic parameters were determined for the nickel complex of naphthalene ( $\eta^2$ - $\text{C}_{10}\text{H}_8$ )  $\text{Ni}(\text{Pr}_2\text{NCH}_2\text{CH}_2\text{NPr}_2)$  [6] and anthracene ( $\eta^2, \eta^2$ -IRHR) [7].

Thermally induced IRHR were found and systematically investigated mainly for chromium tricarbonyl complexes with PAL, in particular, for naphthalene **1a**  $\rightleftharpoons$  **1b** [8–10] (Scheme 1), biphenyl **2a**  $\rightleftharpoons$  **2b** [11] (Scheme 2), and some other ligands (e.g. in biphenylene [12] and dibenzothiophene [13]) by *selective introduction* of substituent R into coordinated aromatic rings. This was achieved by lithiation and further reaction of lithium salt with an electrophile RX (in contrast to fluoranthene, where such approach failed [14]). After such labeling procedure activation barriers could be determined simply and reliable enough by conventional kinetic methods. In complexes dissolved in inert, noncoordinating sol-

vents (e.g. decane or  $\text{C}_6\text{F}_6$ ), during IRHR  $\text{Cr}(\text{CO})_3$  moves *intramolecularly* along the  $\pi$ -system of the ligand between different aromatic rings at 80–170 °C with the activation barrier of ca. 27–33  $\text{kcal mol}^{-1}$  ( $\eta^6, \eta^6$ -rearrangements). The later was proved by the fact that IRHR proceed in inert noncoordinating  $\text{C}_6\text{F}_6$  [9] or even in melt [14], by cross-experiment [15] as well as by the retention of stereochemistry [16] and optical activity [17] in the course of IRHR. Rearrangements proceeding at such rates were monitored by the methods of stationary kinetics (mainly by NMR [9,13–15] and in some cases by HPLC [17] and IR [18]).

## 2. Results and discussions

In this paper, we summarize part of our research on dynamic effects and reactions in chromium tricarbonyl complexes of PAL by DFT. Very modest calculation expenditures [19] provides results qualitatively similar to the results of *ab initio* calculations (which take into consideration the electronic correlation). We used a routine developed by Laikov [20] based on generalized gradient approximation for the nonempirically constructed PBE functional [21]. The one-electron wave functions were expanded in the extended TZ2P atomic basis sets of the contracted Gauss functions such as {311/1}, {6,11111/411/11}, {6111111111/5111111/11}, and {611111111111/5111111111/51111} for the H, C, S, and Cr atoms, respectively. All structures were fully optimized. Corrections for zero-point energies were calculated in the harmonic approximation. The stationary

Table 2

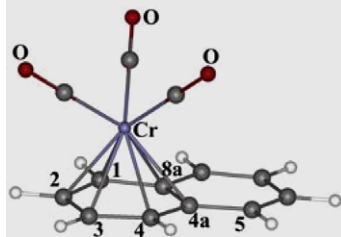
Electron density ( $\rho$ ), Laplacian ( $\nabla^2/\rho_{\text{BCP}}$ ) and ellipticity of electron density ( $\varepsilon$ ) in some critical points for  $\eta^6\text{-C}_{10}\text{H}_8\text{Cr}(\text{CO})_3$  (**1-Pr**).

Bond	$\rho \cdot 10^3$ ( $\text{e au}^{-3}$ )	$\nabla^2 \rho_{\text{BCP}} \cdot 10^3$ ( $\text{e au}^{-5}$ )	$\varepsilon$
BCP(Cr–C1)	62.42	185.7	2.69
BCP(Cr–C2)	63.32	198.7	8.01
BCP(Cr–C3)	63.29	198.7	8.80
BCP(Cr–C4)	62.46	185.7	2.62
RCP(C1–Cr–C2)	61.65		
RCP(C2–Cr–C3)	63.17		
RCP(C3–Cr–C4)	61.65		
RCP(C4a–Cr–C8a)	46.67		
RCP(C1–C2–C3–C4–C4a–C8a)	28.13		
CCP	28.11		

Table 1

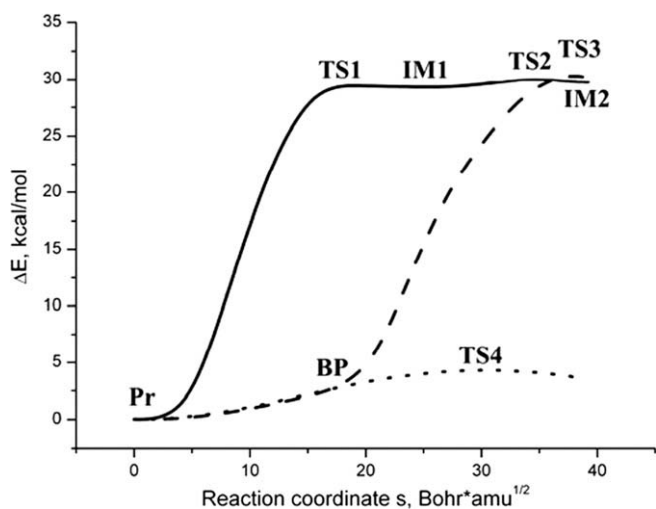
Comparison of calculated and experimental structural parameters for some chromium carbonyl complexes.

Molecule, experimental method	Parameter	Calculation	Experiment	Deviation
$[(\eta^6\text{-C}_{10}\text{H}_8)\text{Cr}(\text{CO})_3]$ , X-ray [25]	Cr–C <sub>CO</sub>	1.847, 1.830	1.815–1.830	0.032
	Cr–C <sub>1</sub>	2.218	2.186, 2.214	0.018
	Cr–C <sub>2</sub>	2.214	2.213, 2.214	0.001
$[(\eta^6\text{-C}_{10}\text{H}_8)\text{Cr}(\text{CO})_3]$ , PCA [25]	Cr–C <sub>4a</sub>	2.336	2.306, 2.337	0.015
	C <sub>2</sub> –C <sub>3</sub>	1.426	1.375	0.051
	C <sub>3</sub> –C <sub>4</sub>	1.405	1.389, 1.383	0.019
	C <sub>4</sub> –C <sub>4a</sub>	1.439	1.447, 1.404	0.014
	C <sub>4a</sub> –C <sub>8a</sub>	1.442	1.439	0.003
	$[\text{Cr}(\text{CO})_6]$ , electronography [26]	Cr–C	1.908	1.924
C–O		1.153	1.165	–0.012



**Table 3**  
Bonds orders for stationary structures for IRHR in **1a** = **1b** (R = H).

Bonds	1-Pr	1-IM1	1-IM2	1-TS1	1-TS2	1-TS3
Cr–C1	0.29					
Cr–C2	0.26	0.06		0.08		
Cr–C3	0.26	0.18	0.08	0.20	0.11	0.08
Cr–C4	0.29	0.41	0.27	0.38	0.32	0.16
Cr–C4a	0.19	0.09	0.18	0.09	0.15	0.25
Cr–C8a	0.19		0.06	0.06	0.05	0.09
Cr–C5			0.27	0.09	0.23	0.16
Cr–C6			0.08		0.06	0.08

**Fig. 1.** Two reaction paths for IRHR **1a** = **1b** (R = H) (RP1 – firm line, RP2 – dotted line) and rotation of Cr(CO)<sub>3</sub> group (RP3 – punctual dotted line) (isolated molecule approximation was used and the difference in the zero-point energy was neglected).

points, viz. prereaction complex (PC), products (Pr), intermediates (IM), and transition states (TS) on the potential energy surface (PES), were determined by analyzing Hessians. Reaction paths were found by the Intrinsic Reaction Coordinate method (IRC) [22]. Ther-

modynamic parameters were calculated using the approximation of restricted rotator and harmonic oscillator at  $T = 298$  K. Energy characteristics such as  $E$  – the total energy of molecular system (MS),  $E^{\circ}$  – the energy with account of ZPVE (zero-point vibration energy), and  $G$  – the free Gibbs energy were used. Charges on the atoms were calculated according to Hirschfeld [23]. All calculations were performed using the MVS 15000BM computer cluster at the Joint Supercomputer Center (JSCC) (Moscow, Russia).

## 2.1. The investigation of the mechanism of interring $\eta^6, \eta^6$ -haptotropic rearrangements in chromium tricarbonyl complexes of PAL by DFT

### 2.1.1. Naphthalenechromiumtricarbonyl $\eta^6\text{-C}_{10}\text{H}_8\text{Cr}(\text{CO})_3$ (**1**)

Minor substituent effects of the group R on the thermodynamic parameters of IRHR (Scheme 1) found earlier *experimentally* [9] for naphthalene species  $\eta^6\text{-C}_{10}\text{H}_7\text{RCr}(\text{CO})_3$  and confirmed by other researchers [10] were quite unexpectedly especially when compared with many other metallotropic rearrangements where these effects are much more pronounced [2]. A reasonable explanation of this finding was obtained in the course of the theoretical investigation of the rearrangement by DFT [9].

However, considerable reducing of calculation expenditures in recent years and some novel results [24] inspired us to reinvestigate some details of IRHR of **1**. It was demonstrated earlier that calculation results reproduce very well experimental structural parameters in chromium complexes of PAL [9,12,13], including such details as differences in Cr–C1(2) and Cr–C4a(8a) bond lengths and even conformation of Cr(CO)<sub>3</sub> group in **1** [25]. Likewise, thermodynamic data are also fit very well with experiment. Results of the calculations on **1** are presented in Tables 1–3.

New investigation of **PES** for IRHR led to two reaction paths (RP) both related to the shift of organometallic group over periphery of naphthalene ligand. First path (RP1) was reported earlier [9] and involves transition state (**1-TS3**) (in which naphthalene ligand is almost flat) without intermediates. The second path (RP2) takes place through two transition states (**1-TS1** and **1-TS2**) and two intermediates (**1-IM1** and **1-IM2**). Second channel of rearrangement was found for the first time in this work. Changes of relative energy along the reaction path in mass-weighted Cartesian coordi-

<b>1-Pr</b> $\Delta E=0; \Delta E^0=0; \Delta G=0$	<b>1-TS3</b> $\Delta E=30.3; \Delta E^0=29.4; \Delta G=28.4$	<b>1-TS1</b> $\Delta E=30.0; \Delta E^0=28.4; \Delta G=28.2$
<b>1-IM1</b> $\Delta E=29.3; \Delta E^0=28.4; \Delta G=26.7$	<b>1-TS2</b> $\Delta E=30.0; \Delta E^0=28.9; \Delta G=28.0$	<b>1-IM2</b> $\Delta E=29.7; \Delta E^0=28.6; \Delta G=26.5$
	<b>1-TS4</b> $\Delta E=4.3; \Delta E^0=4.1; \Delta G=5.2$	

**Fig. 2.** Top view on the stationary structures located on RP1, RP2 and RP3 and their relative energies (kcal mol<sup>-1</sup>).

nates for both processes and  $\text{Cr}(\text{CO})_3$  group rotation (RP3) are presented in Fig. 1.

A flat section of RP1 curve is related to the rotation of  $\text{Cr}(\text{CO})_3$  ( $\sim 30^\circ$ ) and an energy increase equals ca.  $3 \text{ kcal mol}^{-1}$ . This section coincides with the corresponding section of RP3 curve for  $\text{Cr}(\text{CO})_3$  rotation via the transition state (**1-TS4**), whereas curve position for which takes place embranchment corresponds to bifurcation point structure (**1-BP**). Steep increase part of the curve relates to the exit of  $\text{Cr}(\text{CO})_3$  to the periphery of the naphthalene ligand. Such an exit is accompanied by a rupture of some bonds and a minor distortion of the planarity of naphthalene bicycle in the course of shifting.

A steep increase part of RP2 (**1-Pr-1-TS1**) corresponds to the  $\text{Cr}(\text{CO})_3$  exit at the periphery of six-membered ring without rotation. Next flat section corresponds to a slight rotation ( $\sim 15^\circ$ ) of  $\text{Cr}(\text{CO})_3$  (**1-TS1-1-IM1**) and a further shift along the periphery to bridging carbon atom between two six-membered cycles (**1-**

**IM1-1-TS2-1-IM2**). Structures of stationary points located on RP1, RP2 and RP3 and their relative energies ( $\text{kcal mol}^{-1}$ ) are presented in Fig. 2.

It is noteworthy that both reaction paths have practically equal activation barriers and further calculations for substituted naphthalene chromium tricarbonyls ( $\eta^6\text{-C}_{10}\text{H}_7$ ) $\text{Cr}(\text{CO})_3$  (Scheme 1) were done for the most straightforward and simplest path RP1. Particularly, the least motion route of  $\text{Cr}(\text{CO})_3$  from one ring to another via the center of the C4a–C8a bond is forbidden due to the loss of bonding interactions between naphthalene ligand and  $\text{Cr}(\text{CO})_3$  [2a].

According to the topological analysis in the frames of quantum theory of Bader [27], the bond type between two atoms in a molecular system could be determined from parameters corresponding to the bond critical point ( $\rho$  – the electron density,  $\nabla^2\rho_{\text{BCP}}$ -Laplacian and  $\varepsilon$  – the ellipticity of electron density). Such analysis

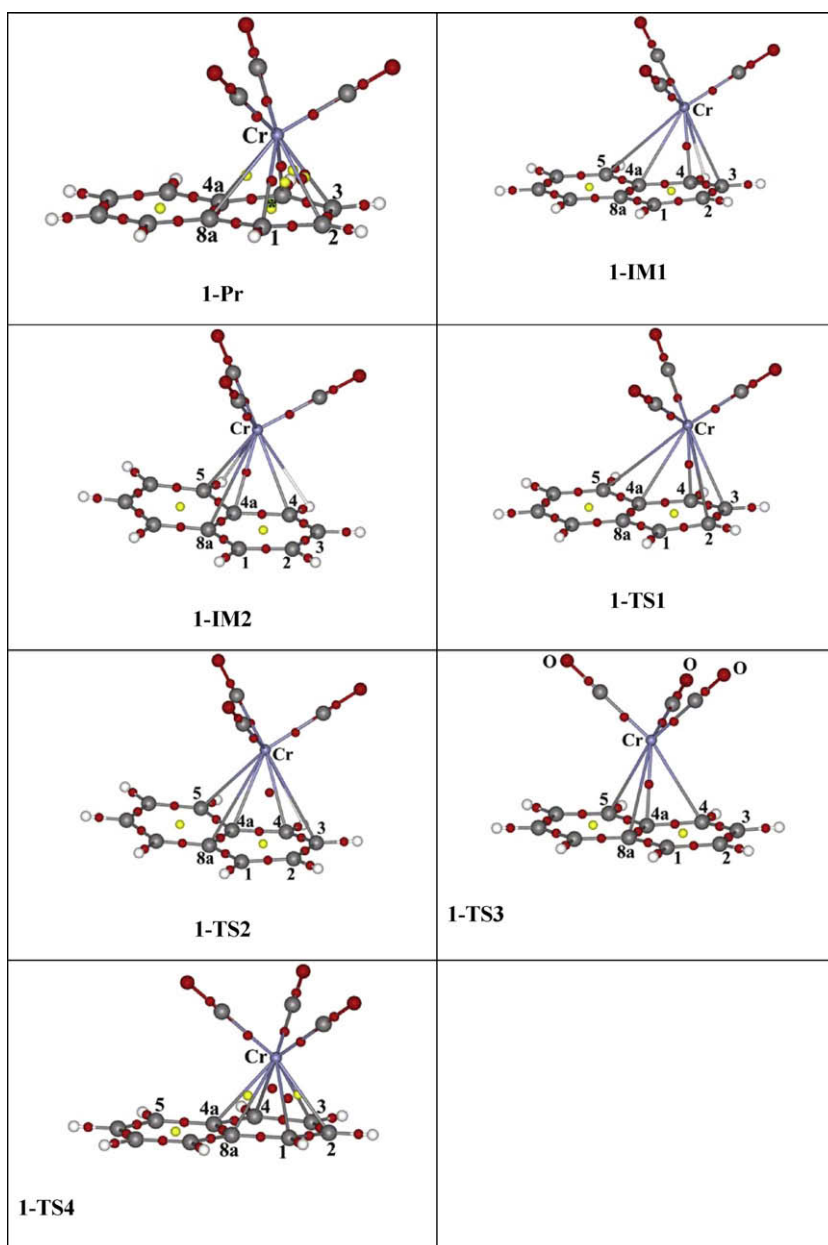
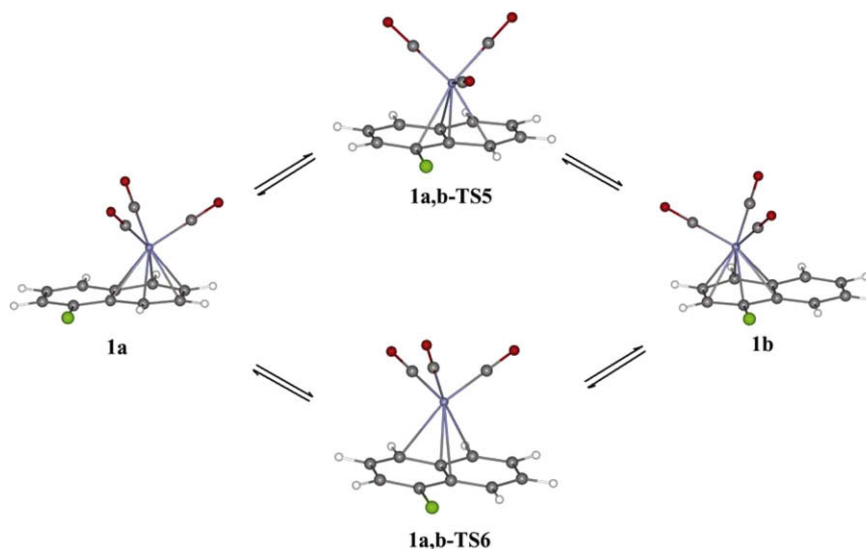


Fig. 3. Critical points: bond critical points (BCP) (solid circles at the center of the bonds), ring critical points (RCP) (bright circles), cage critical points (CCP) (circle with asterisk, **1-Pr**).



Scheme 3.

allowed us to formulate more precisely the hapticity of stationary structures. Structures with calculated critical points are presented in Fig. 3.

From a very formal analysis of BCP one can conclude that **Pr** has an  $\eta^4$ -structure, stationary points **1-IM1**, **1-IM2**, **1-TS1**, **1-TS2**, **1-TS3** have an  $\eta^1$ -structure and **1-TS4** has an  $\eta^2$ -structure. However, such simplified interpretation of the  $\text{Cr}(\text{CO})_3$  coordination is inconsistent with the true bonding and hapticity in chromium tricarbonyl complexes of PAL. There is a lack of BCP(Cr–C4a) and BCP(Cr–C8a) in **Pr** which is a consequence of collapse of these points with RCP(C4–Cr–C4a) and RCP(C1–Cr–C8a) points, correspondingly. The remaining RCP(C4a–Cr–C8a) with  $\rho = 0.04667 \text{ e au}^{-3}$  (Table 2) proves the fact that the electron density in the domain of Cr–C4a and Cr–C8a bonds exceeds  $\rho = 0.04667 \text{ e au}^{-3}$ . Thus, the conventional formulation for this complex as  $\eta^6$  is confirmed. It is worthwhile to note that RCP of coordinated six-membered ring (C1–C2–C3–C4–C4a–C8a) and a single CCP almost collapse (their electron densities are differ by only  $0.02 \text{ e au}^{-3}$ ).

From the data on bond orders (Table 3) and taking into consideration that **Pr** has an  $\eta^6$ -structure, one can assume that significant for existing of Cr–C bond will be the value equal 0.15 or higher. This means that **1-IM1** and **1-TS1** are coordinated  $\eta^2$ , and **1-IM2**, **1-TS2** and **1-TS3** have allyl  $\eta^3$ -structure which is in accordance with the result of Hoffmann [2a].

As was already mentioned above, for the sake of simplicity for substituted naphthalene chromium tricarbonyls the focus was on

Table 4

Relative energies ( $\Delta E$ ) for isomeric complexes and transition states ( $\text{kcal mol}^{-1}$ ) for IRHR **1a**  $\rightleftharpoons$  **1b** (Scheme 3, note that only  $\alpha$ -substituents is depicted on Scheme 3)<sup>a</sup>

	Complex <b>1a</b>	Complex <b>1b</b>	Transition state <b>1a,b-TS5</b>	Transition state <b>1a,b-TS6</b>
R = $\alpha$ -Cl	0	2.78	33.93	30.82
R = $\beta$ -Cl	0	2.22	30.23	30.91
R <sup>b</sup> = $\alpha$ -SiMe <sub>3</sub>	0	-1.64	29.59	30.63
R <sup>b</sup> = $\beta$ -SiMe <sub>3</sub>	0	-4.47	26.41	26.62
R = $\alpha$ -Me	0.52	0	32.18	30.38
R = $\beta$ -Me	-0.19	0	28.86	29.92

<sup>a</sup> Isolated molecule approximation was used and the difference in the zero-point energy was ignored.

<sup>b</sup> Calculations were not done for the complexes with SnMe<sub>3</sub> substituent due to a priori close resemblance of the result with corresponding result for SiMe<sub>3</sub> substituent.

the reaction path of the type RP1 with only one transition state of the type **1-TS3** (Figs. 1 and 2).

There are two different unsymmetrical reaction channels for transfer of the  $\text{Cr}(\text{CO})_3$  between unsubstituted and substituted rings (Scheme 3) via transition states **1a,b-TS5** and **1a,b-TS6**. The calculation reproduces quite well the relative stabilities of isomers differing in the  $\text{Cr}(\text{CO})_3$  group position with respect to the unsymmetrically substituted naphthalene ligand. This leads to excess of one of the isomers in the course of reaction of substituted naphthalene with chromium carbonyls (isomer ratio [**1a**]/[**1b**], Scheme 1) [9]. Substituent variations affect most strongly the energy of transition state **1a,b-TS5** for the substituent in position 2. In general,

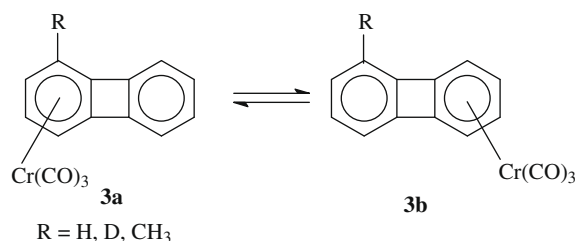
Table 5

Rate and equilibrium constants for **1a**  $\rightleftharpoons$  **1b** in the complexes  $\eta^6\text{-C}_{10}\text{H}_7\text{RCr}(\text{CO})_3$  in solution of  $\text{C}_6\text{F}_6$  at 85 °C [2].

Substituent	$k_1 \cdot 10^5 \text{ (s}^{-1}\text{)}$	$k_2 \cdot 10^5 \text{ (s}^{-1}\text{)}$	$K_{\text{eq}}$	$\Delta G_{358}^\ddagger \text{ (kcal mol}^{-1}\text{)}$
1-CH <sub>3</sub>	0.90 ± 0.01	0.51 ± 0.02	1.77	29.4 ± 0.6
2-CH <sub>3</sub>	1.82 ± 0.10	1.01 ± 0.10	1.80	29.2 <sup>a</sup>
2-CH <sub>3</sub>	3.02 ± 0.24	1.45 ± 0.07	2.09	28.5 ± 1.2
1-Si(CH <sub>3</sub> ) <sub>3</sub>	2.40 ± 0.02	0.50 ± 0.02	4.80	28.7 ± 0.7
2-Si(CH <sub>3</sub> ) <sub>3</sub>	1.93 ± 0.03	0.11 ± 0.01	17.26	29.1 ± 0.6
1-Sn(CH <sub>3</sub> ) <sub>3</sub>	0.70 ± 0.01	0.14 ± 0.01	5.00	29.5 ± 0.5
2-Sn(CH <sub>3</sub> ) <sub>3</sub>	2.24 ± 0.04	0.17 ± 0.01	13.26	28.8 ± 0.7
1-Cl	0.15 ± 0.01	4.36 ± 0.06	0.034	30.6 ± 0.4
2-Cl	0.40 ± 0.01	3.46 ± 0.06	0.12	30.2 ± 0.8
2-D <sup>b</sup>	0.38 ± 0.02	0.38 ± 0.02	1.00	30.4 ± 0.8

<sup>a</sup> Calculation based on the data of Kündig et al. [10a].

<sup>b</sup> Data for IRHR of deuterated complexes starting from complex where deuterium is in position 2 of coordinated ring (Scheme 1).

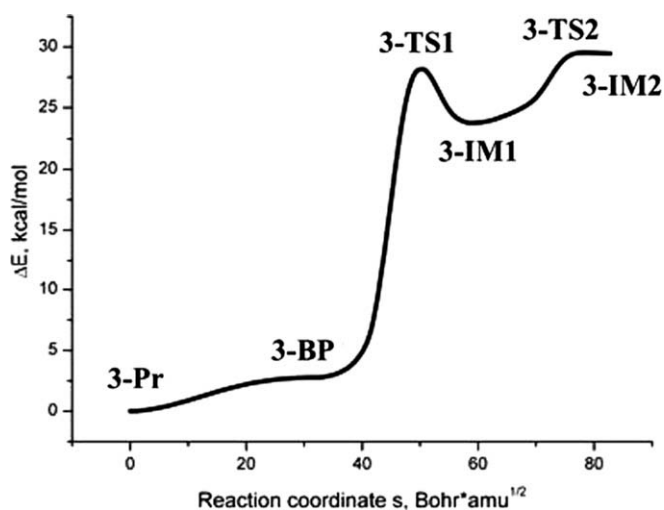


Scheme 4.



**Table 6**Relative energies and inter-atomic distances for stationary points on the potential energy surface of degenerate rearrangement **3a**  $\rightleftharpoons$  **3b** (R =  $\alpha$ -H).

Parameters	<b>3-Pr</b>	<b>3-BP</b>	<b>3-TS1</b>	<b>3-IM1</b>	<b>3-TS2</b>	<b>3-IM2</b>
$\Delta G$ (kcal mol <sup>-1</sup> )	0	4.5	27.1	22.7	28.5(32.24) <sup>a</sup>	26.7
R(Cr–C1)	2.262 (2.249) <sup>a</sup>	2.254	2.556	2.662	3.443	3.578
R(Cr–C2)	2.195 (2.199) <sup>a</sup>	2.210	2.950	3.295	3.797	3.917
R(Cr–C3)	2.195 (2.199) <sup>a</sup>	2.210	2.950	3.295	3.451	3.538
R(Cr–C4)	2.262 (2.249) <sup>a</sup>	2.254	2.556	2.662	2.621	2.672
R(Cr–C5)	2.252 (2.229) <sup>a</sup>	2.222	2.210	2.161	2.163	2.200
R(Cr–C6)	2.252 (2.229) <sup>a</sup>	2.222	2.210	2.161	2.607	2.702
R(Cr–C11)	3.345	3.324	2.755	2.314	2.247	2.200
R(Cr–C12)	3.345	2.222	2.755	2.314	2.673	2.702
R(Cr–C14)	4.546	4.524	3.808	3.367	2.829	2.672

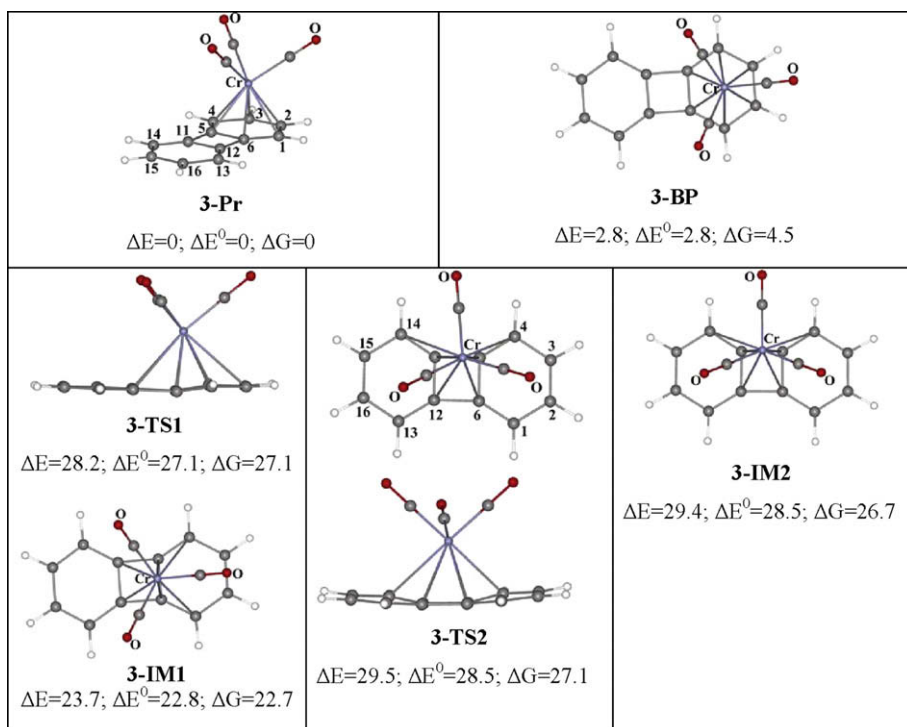
<sup>a</sup> Experimental data,  $\Delta G_{403}^{\#} = 32.24$  kcal mol<sup>-1</sup> for **3a**  $\rightleftharpoons$  **3b** (R =  $\alpha$ -D) [12].**Fig. 4.** Reaction paths for IRHR **3a**  $\rightleftharpoons$  **3b** (R = H) (isolated molecule approximation was used and the difference in the zero-point energy was ignored).

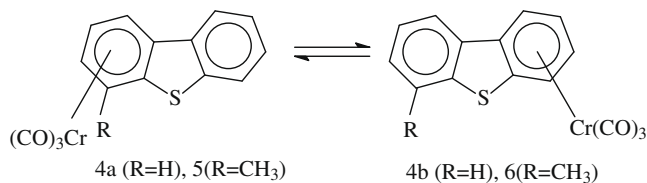
the energies of transition states **1a,b-TS6** change only slightly ( $\pm 1$  kcal mol<sup>-1</sup>), except for the 2-Me<sub>3</sub>Si substituent. The existence of two reaction channels one of which is practically unperturbed, determines only a slight sensitivity of the *experimental* rearrangement rate to the ligand substitution. Considering the inherent approximations (approximation of the isolated molecule, neglecting the difference in energies of zero vibration), the calculated activation barriers are in a good agreement with the experimentally determined  $\Delta G^{\#}$  values (cf. data in Tables 4 and 5 and Scheme 3).

### 2.1.2. Biphenylenechromiumtricarbonyl $\eta^6$ -C<sub>12</sub>H<sub>8</sub>Cr(CO)<sub>3</sub> (**3**)

A reasonable resemblance with experimental barrier  $\Delta G_{403}^{\#} = 32.24$  kcal mol<sup>-1</sup> for  $\eta^6, \eta^6$ -IRHR **3a**  $\rightleftharpoons$  **3b** (R = D) was obtained in a detailed mechanistic investigation of the rearrangement by DFT (Scheme 4).

Earlier theoretical data [12] for **3** were reinvestigated with the emphasis on the mechanistic details of IRHR. The results of calculations agree with experimental structural parameters in  $\eta^6$ -biphenylene chromium tricarbonyl **3**, including differences in the Cr–C bond lengths with coordinated ring carbons and the

**Fig. 5.** Top and side view on the stationary structures on the potential energy surface of degenerate rearrangement **3a**  $\rightleftharpoons$  **3b** (R =  $\alpha$ -H) and their relative energies (kcal mol<sup>-1</sup>).



conformation of the  $\text{Cr}(\text{CO})_3$  in the ground state. Activation barrier for IRHR  $\mathbf{3a} \rightleftharpoons \mathbf{3b}$  ( $\text{R} = \alpha\text{-H}$ ) agrees also with the experimental kinetic results. Data are presented in Table 6 and in Figs. 4 and 5. In contrast to IRHR in  $\mathbf{1}$  where the transition states were practically flat, there is a considerable deviation from planarity in both IRHR transition states of  $\mathbf{3}$ .

Considering the inherent approximations (approximation of the isolated molecule, neglecting the difference of energies of zero vibration), the calculated activation barrier well agrees with the experimentally determined  $\Delta G^\ddagger$ .

### 2.1.3. Dibenzothiophenechromiumtricarbonyl $\eta^6\text{-C}_{12}\text{H}_8\text{SCr}(\text{CO})_3$ ( $\mathbf{4}$ )

The mechanism of degenerate inter-ring haptotropic migration for  $\mathbf{4}$  of the metal-containing group (Scheme 5,  $\text{R} = \text{H}$ ,  $\mathbf{4a} \rightleftharpoons \mathbf{4b}$ ) was theoretically studied by DFT. A quantum chemical analysis of the potential energy surface (PES) (Fig. 6) of the degenerate haptotropic rearrangement  $\text{Cr}(\text{CO})_3$  from the ground state  $\mathbf{4-Pr}$ , i.e. from one benzene ring to another, demonstrated that the reaction proceeds through the  $\mathbf{4-IM}$  intermediate, where  $\text{Cr}(\text{CO})_3$  is coordi-

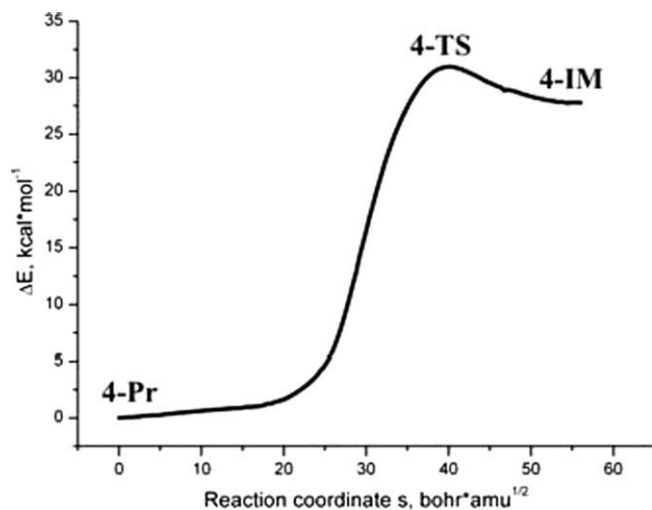


Fig. 6. Calculated reaction coordinates of the IRHR rearrangement  $\mathbf{4a} \rightleftharpoons \mathbf{4b}$  in mass-weighted Cartesian coordinates (isolated molecule approximation was used and the difference in the zero-point energy was ignored).

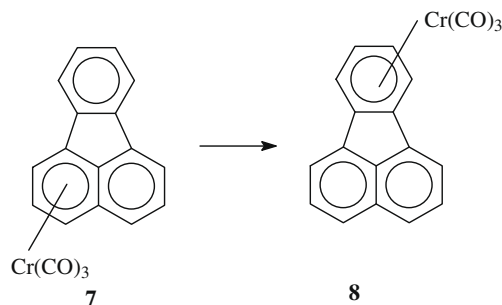
Table 7  
Geometric parameters of stationary points for IRHR  $\mathbf{4a} \rightleftharpoons \mathbf{4b}$  ( $\text{R} = \text{H}$ ).

Distance, r/Å	4-Pr	4-Im	4-TS
Cr–C(1)	2.213	2.608	2.379
Cr–C(2)	2.213	3.551	2.961
Cr–C(3)	2.205	4.085	3.416
Cr–C(4)	2.230	3.886	3.343
Cr–C(4a)	2.292	3.029	2.748
Cr–C(9)	4.400	2.608	3.355
Cr–C(9a)	3.436	2.261	2.711
Cr–C(9b)	2.298	2.261	2.216
Cr–CO	1.847, 1.847, 1.837	1.822, 1.822, 1.806	1.812, 1.818, 1.806
Cr–S	3.718	3.727	3.750
C–O	1.166	1.172	1.172

nated to four peripheral carbon atoms to form an  $\eta^4$ -pseudodiene complex. The reaction path links the product with an intermediate through transition state  $\mathbf{4-TS}$  (Fig. 7). The structure of the latter intermediate corresponds to the structure of a distorted  $\eta^4$ -trimethylenemethane complex. The interatomic distances in the ground state, the intermediate, and the transition state are given in Table 7. The relative energy of the intermediate with regard to ground (basic) state is  $27.3 \text{ kcal mol}^{-1}$ . Taking into account the zero-point energy, the barrier equals  $31.2 \text{ kcal mol}^{-1}$ . This agrees well the experimental barrier of  $32.24 \text{ kcal mol}^{-1}$  measured for  $\mathbf{5} \rightleftharpoons \mathbf{6}$  IRHR involving a 1-methylsubstituted complex [13].

### 2.1.4. Fluoranthenechromiumtricarbonyl $\eta^6\text{-C}_{16}\text{H}_{10}\text{Cr}(\text{CO})_3$ ( $\mathbf{7}$ ) and ( $\mathbf{8}$ )

Earlier it was shown that reactions of fluoranthene with  $\text{Py}_3\text{Cr}(\text{CO})_3/\text{BF}_3 \cdot \text{OEt}_2$  or  $(\text{CH}_3\text{CN})_3\text{Cr}(\text{CO})_3$  at 25 and 50 °C, respectively, under kinetic control conditions mainly gave  $[\eta(6\text{-}10,16)\text{fluoranthene}]\text{Cr}(\text{CO})_3$   $\mathbf{7}$ . On the contrary, its interaction with  $\text{Cr}(\text{CO})_6$  in boiling  $\text{Bu}_2\text{O}$  at 130 °C (thermodynamic control conditions) resulted in the formation of only  $[\eta(1\text{-}5,15)\text{fluoranthene}]\text{Cr}(\text{CO})_3$   $\mathbf{8}$ . Complex  $\mathbf{7}$  isomerizes irreversibly into  $\mathbf{8}$  at temperatures above 90 °C; the isomerization proceeded as IRHR  $\mathbf{7} \rightarrow \mathbf{8}$  in  $\text{C}_6\text{F}_6$  with  $\Delta G^\ddagger = 32.6 \text{ kcal mol}^{-1}$  (Scheme 6) [14]. In order to reveal a deeper insight into the mechanisms of this transformation, a theoretical



Scheme 6.

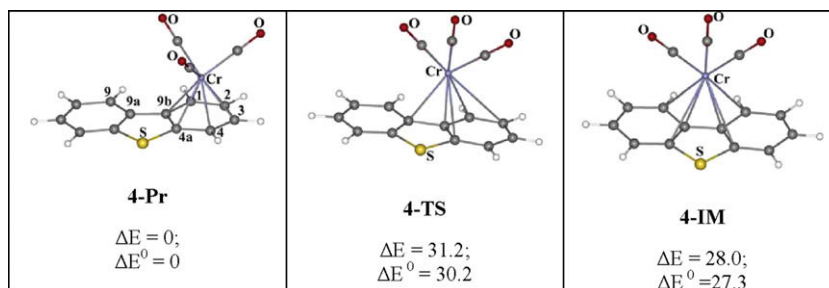


Fig. 7. Stationary structure of the IRHR  $\mathbf{4a} \rightleftharpoons \mathbf{4b}$  and their relative energies ( $\text{kcal mol}^{-1}$ ).

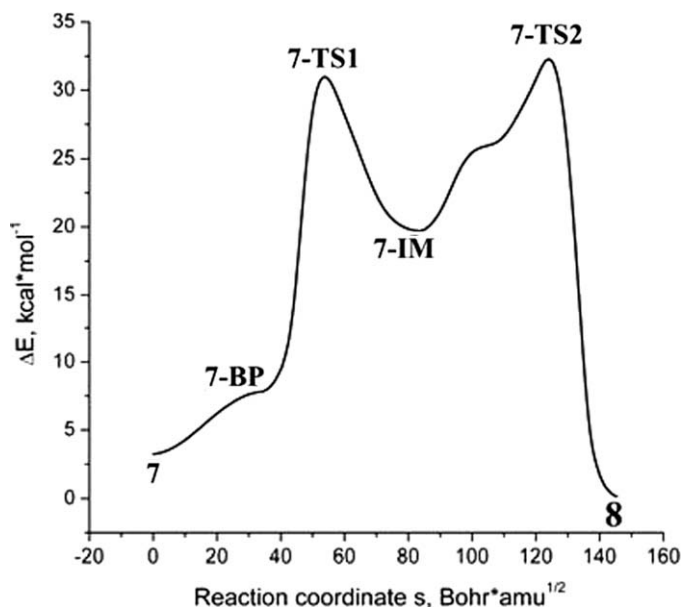


Fig. 8. Relative energy along reaction coordinate of IRHR **7** → **8** (isolated molecule approximation was used and the difference in the zero-point energy was ignored).

study of the structure of isomeric complexes **7** and **8** and the mechanism of the interring haptotropic rearrangement was performed by DFT (Fig. 8).

The results of calculation agreed with experimental data. The energy of **8** was by 3 kcal mol<sup>-1</sup> lower than that of **7**. The global

Table 8

Calculated (A) and experimental (B) C–C bond lengths (Å) in the ligand and complexes **7**, **8** and **8a** in the ground state.

Bond	<b>7</b>		<b>8a</b>		Fluoranthene		<b>8</b>
	A	B[14]	A	B[1]	A	B <sup>a</sup>	A
r(C1–C2)	1.398	1.381	1.412	1.392	1.402	1.386	1.427
r(C1–C15)	1.397	1.389	1.422	1.416	1.394	1.384	1.406
r(C2–C3)	1.402	1.388	1.427	1.416	1.400	1.379	1.411
r(C3–C4)	1.399	1.396	1.412	1.389	1.402	1.373	1.427
r(C4–C5)	1.395	1.381	1.422	1.408	1.394	1.388	1.406
r(C5–C6)	1.472	1.476	1.473	1.471	1.475	1.476	1.473
r(C5–C15)	1.431	1.421	1.442	1.426	1.432	1.417	1.459
r(C6–C7)	1.407	1.400	1.385	1.368	1.385	1.367	1.385
r(C6–C16)	1.437	1.423	1.417	1.407	1.419	1.411	1.418
r(C7–C8)	1.434	1.430	1.422	1.414	1.423	1.411	1.420
r(C8–C9)	1.413	1.398	1.389	1.366	1.389	1.368	1.389
r(C9–C10)	1.444	1.439	1.425	1.413	1.425	1.422	1.423
r(C10–C11)	1.428	1.424	1.425	1.420	1.425	1.423	1.424
r(C10–C16)	1.414	1.407	1.406	1.396	1.406	1.400	1.409
r(C11–C12)	1.386	1.364	1.389	1.362	1.389	1.360	1.389
r(C12–C13)	1.423	1.428	1.422	1.414	1.423	1.407	1.420
r(C13–C14)	1.384	1.369	1.385	1.371	1.385	1.372	1.385
r(C14–C15)	1.468	1.474	1.472	1.471	1.475	1.476	1.472
r(C14–C16)	1.427	1.422	1.417	1.408	1.419	1.411	1.418

<sup>a</sup> A.C. Hazell, D.W. Jones, J.M. Sowden, Acta Crystallogr. Sect. B: Struct. Sci. 33 (1977) 1516.

minimum corresponds to complex **8** with the *endo*-conformation of chromium tricarbonyl group. A higher by 0.3 kcal mol<sup>-1</sup> local minimum corresponds to *exo*-conformer **8a** (Fig. 9). Rotations around the metal–ligand bond occur via transition state **8-TS(r)** (in which the Cr(CO)<sub>3</sub> group is rotated by 30°) with a low barrier of 0.4 kcal mol<sup>-1</sup>. According to the X-ray structure data [14], com-

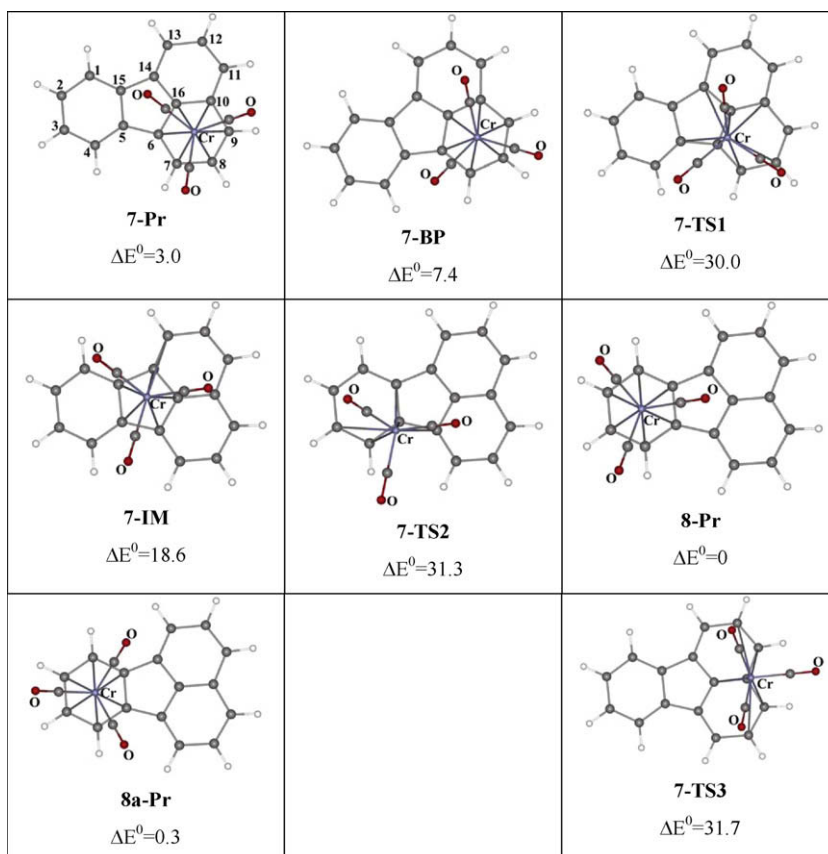


Fig. 9. Top and side view on the stationary structures and relative energies ( $\Delta E^0$ , kcal mol<sup>-1</sup>) on the potential energy surface of IRHR **7** → **8** and degenerate IRHR **7** ⇌ **7'** (see below).



**Table 9**  
Distances Cr–C(*n*) (Å) in stationary structures **7**, **8**, **8a** and **7-BP** and **8-TS(r)**.

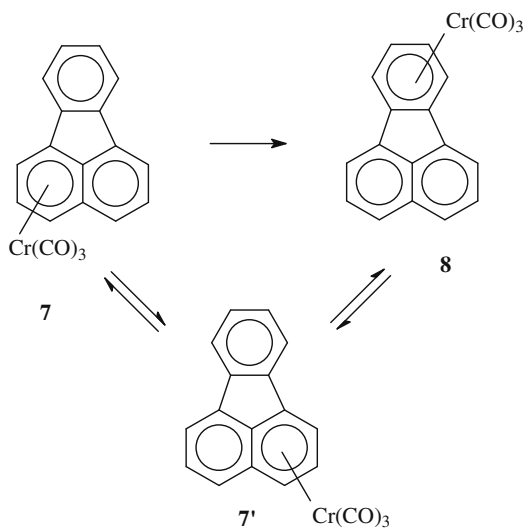
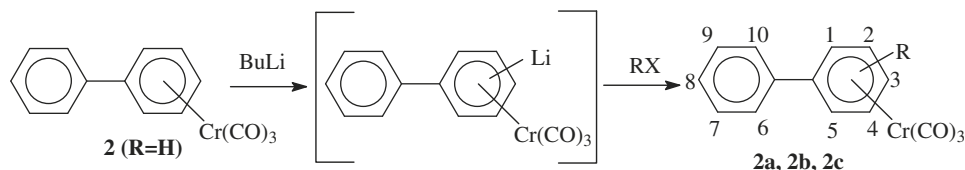
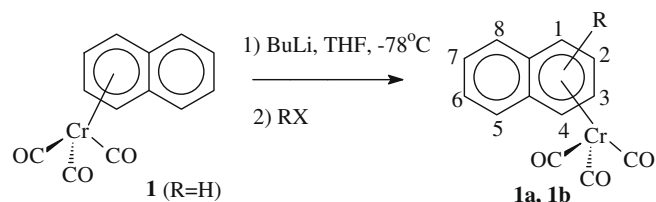
C( <i>n</i> )	<b>7</b>	<b>7-BP</b>	C( <i>n</i> )	<b>8</b>	<b>8a</b>	<b>8-TS(r)</b>
C6	2.272 (2.240) <sup>a</sup>	2.262	C1	2.239	2.232 (2.235)	2.224
C7	2.230 (2.225)	2.243	C2	2.215	2.215 (2.203)	2.228
C8	2.203 (2.204)	2.208	C3	2.214	2.215 (2.209)	2.206
C9	2.212 (2.221)	2.238	C4	2.241	2.215 (2.209)	2.206
C10	2.340 (2.306)	2.307	C5	2.265	2.265 (2.259)	2.264
C16	2.303 (2.272)	2.271	C15	2.265	2.265 (2.243)	2.274

<sup>a</sup> Experimental X-ray values from [14] are given in parentheses.**Table 10**  
Distances Cr–C(*n*) (Å) of calculated transition states **7-TS1**, **7-TS2** and **7-TS3** on the potential energy surface.

C( <i>n</i> )	<b>7-TS1</b>	C( <i>n</i> )	<b>7-TS2</b>	C( <i>n</i> )	<b>7-TS3</b>
C5	2.835	C4	2.378	C9	2.505
C6	2.188	C5	2.205	C10	2.171
C7	2.465	C6	2.776	C11	2.507
C16	2.414	C15	2.694	C16	2.654

plex **8** exists as an exo-conformer **8a** in crystals. This can be caused by packing effects in the crystalline state. A comparison of the calculated geometric parameters for **7** and **8a** with the X-ray structure data (Tables 8 and 9) revealed that our calculations reproduce correctly all principal experimental tendencies, such as an increase in C–C bond lengths in the coordinated ring and the alternation of long and short bonds. The calculated C–C and Cr–C bond lengths are systematically exaggerated by 0.01–0.02 Å when compared with the X-ray structure data. This corresponds to the accuracy of density functional calculations.

Unlike **8**, complex **7** is characterized by a substantial rotational (7.4 kcal mol<sup>-1</sup>) barrier of the Cr(CO)<sub>3</sub> group. The potential energy

**Scheme 7.****Scheme 8.**1-R, 2-R, (R = D, Me, Me<sub>3</sub>Si, Me<sub>3</sub>Sn etc.)**Scheme 9.**

surface for this rotation contains a single nondegenerate conformer **7** and a saddle point **7-BP** (Figs. 8 and 9). The specific feature of the **7-BP** as a transition state consists in that in this point Cr(CO)<sub>3</sub> group rotates by 60° as compared to its orientation in **7** (for the process of rotation **7-BP** is saddle point) and reaction coordinate bifurcates on rotation and haptotropic rearrangement **7** → **8**, see below.

### 2.1.5. The interring nondegenerate haptotropic rearrangement **7** → **8**

The reaction path for the interring haptotropic rearrangement **7** → **8** (Fig. 8) is divided into three steps. The Cr(CO)<sub>3</sub> group rotates first (**7** → **7-BP**) followed by a shift via transition state **7-TS1** into intermediate **7-IM**, and, finally into **8** via **7-TS2** (Fig. 9). As in other interring haptotropic rearrangements studied earlier, Cr(CO)<sub>3</sub> moves through transition states along the periphery of the ring. The potential of the third region has a small flattening in the middle, a “step” where the reaction path turns from the center of the five-membered ring to the periphery. As a consequence, the potential barrier width increases in this region. Note that **7-TS1** and **7-TS2** have structures close to η<sup>4</sup>-type complexes (see Table 10).

### 2.1.6. Degenerate haptotropic rearrangement in **7**

In addition to the interring haptotropic rearrangement **7** → **8**, the degenerate rearrangement in **7** between two equivalent six-membered rings of the naphthalene fragment is theoretically possible. According to DFT calculation, such a displacement of the Cr(CO)<sub>3</sub> occurs through *symmetric* transition state **7-TS3**, in which Cr(CO)<sub>3</sub> is coordinated to the peripheral C9, C10, C11, and C16 atoms (Fig. 9). As for the degenerate haptotropic rearrangement in (η<sup>6</sup>-naphthalene)Cr(CO)<sub>3</sub>, the calculated activation barrier for this rearrangement was in a close agreement with Δ*G*<sup>#</sup> determined experimentally (28.9–33.9 kcal mol<sup>-1</sup>, Table 5). In complex **7**, there is a second route for the Cr(CO)<sub>3</sub> transfer during the degenerate interring haptotropic rearrangement through the five-membered ring, namely, **7** → **7-TS1** → **7-IM** → **7-TS1'** → **7'** (**7-TS1'** and **7'** have *mirror symmetry* relative to **7-TS1** and **7**, respectively). This route is energetically more favorable because the **7-TS1** transition state, which has the highest energy along this route, lies by 7 kcal mol<sup>-1</sup> below **7-TS3**.

So far current attempts to selectively label complex **7** and to measure experimentally the activation barrier for this degenerate rearrangement between two six-membered rings in naphthalene fragment of **7** failed. Experiments are on the way to resolve enan-

**Table 11**

Yields and selectivity of the reactions of the lithium salts of tricarbonyl- $\eta^6$ -biphenyl- and tricarbonyl- $\eta^6$ -naphthalenechromium with electrophilic agents at  $-78^\circ\text{C}$  in THF (**a**, **b**, **c** – positions 1, 2, 3 correspondingly).

RX	Yield of <b>1a+1b</b> (%)	Ratio <b>1a:1b</b>	Yield of <b>2a + 2b + 2c</b> (%)	Ratio <b>2a:2b:2c</b>
D <sub>2</sub> O	87	44:56	84	10:65:25
CH <sub>3</sub> I	66	36:64	18	12:58:30
Me <sub>3</sub> SnCl	74	30:70		
Me <sub>3</sub> SiCl	45	34:76		
I <sub>2</sub>	20	<sup>a</sup>		

<sup>a</sup> Only isomer **1b** is formed.

tiomers of **7** (R- and S-isomers, correspondingly) by HPLC by using optically active column and to investigate the kinetics of both IRHR **7**  $\rightleftharpoons$  **8** and **7**  $\rightleftharpoons$  **7'** (the latter via loss of the optical activity; see Scheme 7).

All our data on DFT analysis of IRHR in chromium tricarbonyl complexes of the investigated PAL presented here are in general agreement with recent publications [24].

## 2.2. Lithiation of tricarbonylchromium complexes with polyaromatic carbo- and heterocyclic ligands. Theoretical DFT study

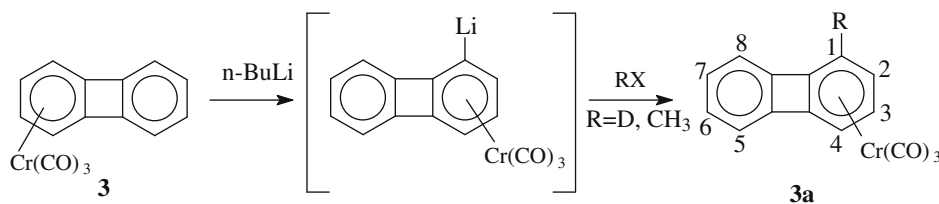
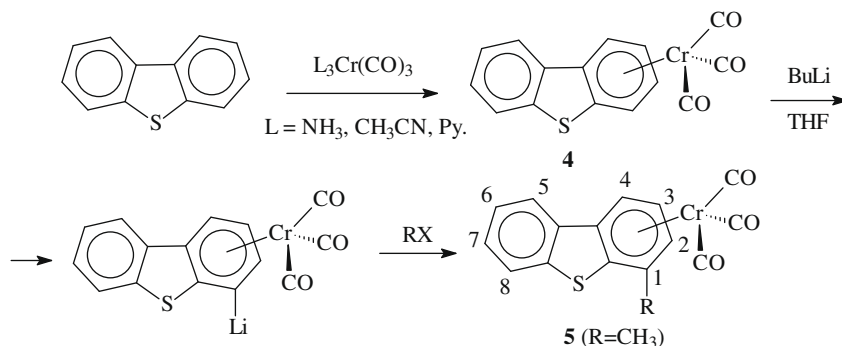
One of the most important synthetic reactions of arenetricarbonylchromium complexes is *lithiation*. It involves replacement of hydrogen by lithium under the action of alkyllithium compounds RLi. Monocyclic complexes react with classical organolithium bases (most frequently, with *n*-butyllithium) at low temperatures ( $\sim -78^\circ\text{C}$ ) in ethereal solvents. The organolithium intermediate further reacts with an electrophilic agent RX (R = D, Me, Me<sub>3</sub>Si, Me<sub>3</sub>Sn, etc.). Depending on the synthetic problem, one can isolate R-substituted complex or under the action of light or an oxidant to obtain R-substituted free ligands. The substituent R in the complex or ligand is located at the same position as lithium. The most important feature of lithiation of the tricarbonylchromium  $\pi$ -complexes with PAL is regioselectivity. Lithiation

occurs at the aromatic ring bonded to the transition metal because  $pK_a$  of the aromatic ring bound to Cr(CO)<sub>3</sub> is nearly seven units lower than that of the noncoordinated moiety [28].

This reaction is important for investigations of the above mentioned IRHR because selective labeling of coordinated ring takes place via initial lithiation of this ring. However, within the metal-coordinated aromatic ring, the formation of lithium–carbon bond is generally nonregioselective. Lithiation followed by the interaction of the lithium derivative of  $\eta^6$ -biphenyltricarbonylchromium **2** (R = H, Scheme 8) with an electrophilic agent (RX = D<sub>2</sub>O, MeI) occurs at all of the three possible positions (*ortho*, *meta*, and *para*) of the coordinated ring, resulting in compounds **2a**, **2b**, and **2c**, respectively (Scheme 8). In general the lithiation of the corresponding tricarbonylchromium complexes of polyaromatic ligands occurs similar. For instance, complex **1** (R = H) is regioselectively metallated at the coordinated aromatic ring. However, if exotic sterically hindered organolithium derivatives are not used for the lithiation of **1** (R = H), no regioselectivity is observed inside the coordinated ring and the interaction with an electrophile RX produces a mixture of  $\alpha$ - and  $\beta$ -R-derivatives **1a** and **1b** with some predominance of the  $\beta$ -isomer (see Scheme 9 and Table 11).

However, the regioselective metallation (BuLi, THF,  $-78^\circ\text{C}$ ) of the tricarbonylchromium complex of carbocyclic biphenylene **3** is also known (Scheme 10). The metallation proceeds exclusively to position 1 to form complex **3a**. Reasons for this difference in regioselectivity between the complexes of biphenylene, on the one hand, and biphenyl and naphthalene, on the other, remain unclear.

The chemistry of the chromium tricarbonyl complexes of arenes changes dramatically in comparison with the first two examples in the presence of a heteroatom (N, S, O, etc.) as a substituent in the coordinated six-membered ring of the complex. In this case, the coordinated ring is metallated exclusively at the *ortho*-position relative to the heteroatom if the substituent creates no significant steric hindrance. It is commonly accepted that this selectivity is due to an additional stabilizing interaction of lithium with heteroatom [29]. It was also previously shown [13] that the lithiation of **4** is regioselective and only compound **5** is produced (R = CH<sub>3</sub>) (Scheme 11).

**Scheme 10.****Scheme 11.**

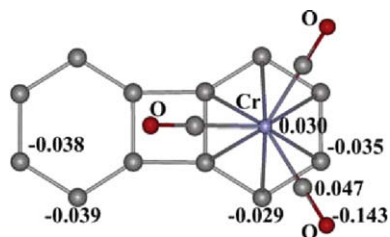


Fig. 10. Charge distribution in a molecule of **3**.

Although the existence of lithium derivatives of arenetricarbonylchromium complexes was reliably proved by IR [2,18] and NMR spectroscopy [18,30], these substances are very unstable and reactive. That prevented their isolation and study by different physico-chemical methods, including X-ray diffraction analysis. To the best of our knowledge, there are no published data on the X-ray determination of the structure of the lithium derivatives of the tricarbonylchromium complexes with aromatic ligands. Nevertheless, simple lithium derivatives of organic mono- and polyaromatic compounds [31], including those containing a heteroatom [32], were intensely studied by different methods (including X-ray diffraction) in both the absence and the presence of additional coordinating ligands (tetramethylethylenediamine, THF, diethyl ether, etc.). Thus, it is evident that alternative, in particular, quantum chemical methods should be used to study the structure and reactivity of lithium derivatives of the arenetricarbonylchromium complexes.

The purpose of this work was to develop the DFT-based calculated criterion for determining the direction of lithiation of the tri-

carbonylchromium complexes of aromatic ligands and to study structures of resulting lithium salts.

Assuming that the interaction of a lithium derivative with an electrophile does not change the site of incorporation of substituent R, replacing the lithium atom, it is necessary to determine a parameter, whose numerical value would show that one of the positions in the coordinated ring of the ligand is preferentially attacked by a molecule of *n*-BuLi. As a result, the lithium atom and then substituent R enter into this position. In this case, this parameter can be considered as a criterion for the direction of metallation. Complex **3** was chosen as a *test compound*, because it is metallated exclusively at position 1 of the coordinated ring. This facilitates considerably data interpretation and the search of the theoretical criterion. In a first stage the optimized electronic structure and negative charge distribution in compound **3** were considered as determining a possible direction of the attack of *n*-BuLi.

The electron density distribution (Fig. 10) calculated by the Hirschfeld method [23] shows that the negative charge is mainly concentrated on the carbonyl groups. Negative charges of carbon atoms of the noncoordinated and coordinated rings are very similar. Therefore, the electron density at different atoms could hardly serve as a criterion for Li<sup>+</sup> localization in the corresponding lithium salt and cannot thus determine the regioselectivity of metallation. Next were calculated the structures and energy parameters of all molecular systems (prereaction complex **PC**, transition state **TSLi**, and reaction products **Pr**), which represent the stationary points on the reaction coordinate of **3** with *n*-butyllithium. The results of calculation for the lithiation of **3** at positions 1, 2, and 5 to form 1-Li-**3**, 2-Li-**3**, and 5-Li-**3** are given (Fig. 11). In all cases, the prereaction complex is a structure with an additional coordination interaction of lithium and oxygen of one of the carbonyl groups.

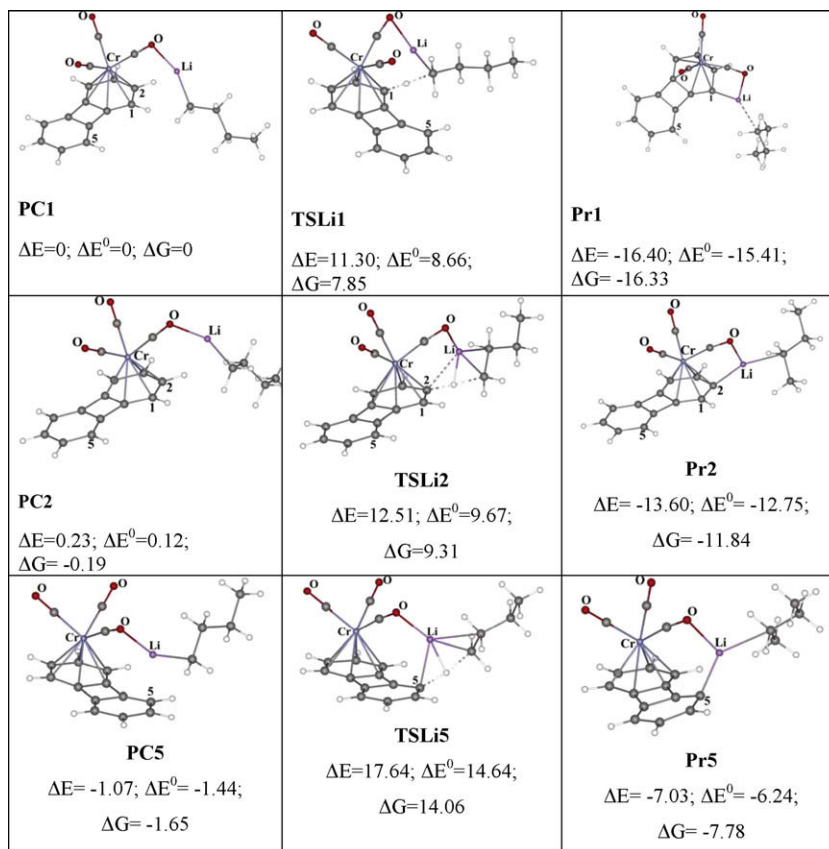
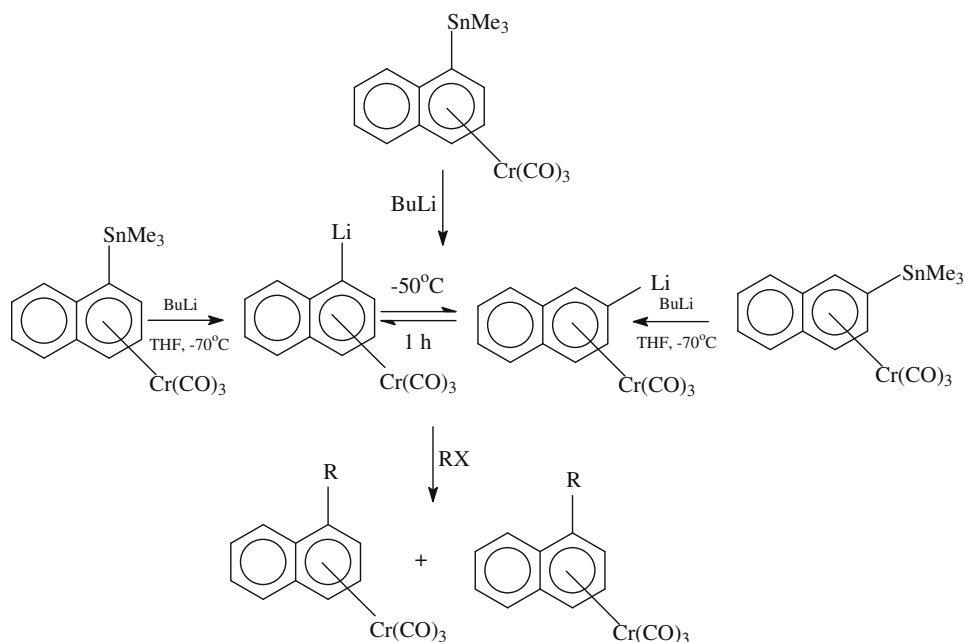


Fig. 11. Data of the DFT calculation of stationary structures **PC**, **TSLi**, and **Pr** for the reaction of **3** with *n*-BuLi at the C(1), C(2), and C(5) atoms, respectively ( $\Delta E$ ,  $\Delta E^0$ , and  $\Delta G$  are the energies relative to **PC1** in kcal mol<sup>-1</sup>).



Scheme 12.

This stabilizing interaction is retained further in the corresponding final lithium derivatives. The interaction of alkaline metal cations with the carbonyl groups in the tricarbonylchromium complexes of aromatic anions is well known and was studied in detail using IR spectroscopy [18]. The transition states exhibit a gradual elongation of the attacked C–H bond. This is followed by the removal of  $H^+$  and its replacement by the  $Li^+$  to form an organolithium derivative and butane. For simplicity of calculations solvent effects were ignored. It is found that the activation barrier of lithiation at positions 1 and 2 of the coordinated ring is  $\sim 9 \text{ kcal mol}^{-1}$  for all types of energies (**TSLi1-PC1** and **TSLi2-PC2**, respectively). This value remains virtually unchanged at different reaction directions (barrier at position 1 is lower than that at position 2 only by  $\sim 1 \text{ kcal mol}^{-1}$ ). For lithiation at position 5 of the noncoordinated ring, the activation barrier is  $\sim 16 \text{ kcal mol}^{-1}$ . Calculation for another noncoordinated ring position 6 gave an increase in the barrier by  $\sim 1 \text{ kcal mol}^{-1}$  (this value is omitted in Table 14). Therefore, the kinetic factor determined by the activation barrier of lithiation predicts the regioselectivity of

metallation at the coordinated ring but is poorly appropriate for predicting the lithiation position in this ring. The relative energies of different types ( $\Delta E$ ,  $\Delta E^\circ$ , and  $\Delta G$ ) for isomeric 1- and 2-lithium derivatives **3** differ more considerably ( $\sim 3 \text{ kcal mol}^{-1}$ ). This indicates that the ratio of the isomers should be determined to a greater extent by the thermodynamic than by kinetic factor. This conclusion is in accordance with the existence of thermodynamic equilibration by means of either inter- and/or intramolecular Li, H-exchange of  $\alpha$ - and  $\beta$ -lithium salts of naphthalene  $Cr(CO)_3$ . Such equilibration is observed after approx. 1 h at temperatures higher than  $-50^\circ\text{C}$  in THF (Scheme 12). It was found experimentally and seems to be a general phenomenon in lithium salts of chromium tricarbonyl complexes in condensed polycyclic aromatics [33].

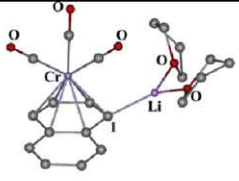
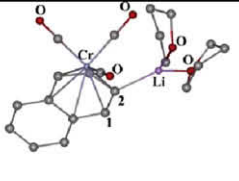
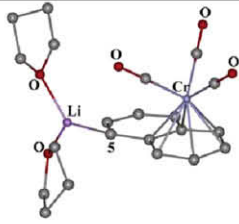
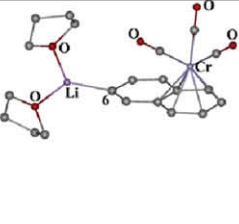
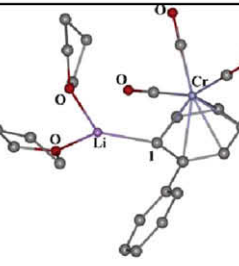
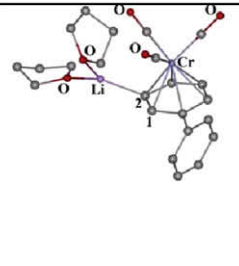
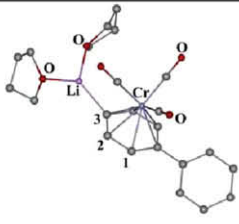
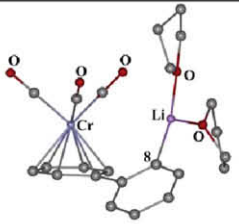
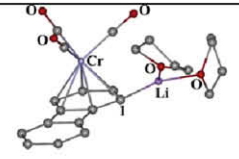
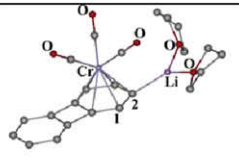
It is possible to simplify significantly further calculations by determining the energy parameters of the reaction products only and ignoring the transition states. Taking into account these facts, as well as considerable errors in the calculation of the free energies  $\Delta G$  in the framework of the program used, the relative energy with

a	b	c	d
$S^0$	$S^1=S^0+THF$	$S^2=S^1+THF$	$S^3=S^2+THF$
$\Delta E=0;$	$\Delta E= -19.41;$	$\Delta E= -12.53;$	$\Delta E= -8.69;$
$\Delta E^0=0;$	$\Delta E^0= -18.62;$	$\Delta E^0= -11.55;$	$\Delta E^0= -8.05;$
$\Delta G=0$	$\Delta G= -7.23$	$\Delta G= -0.74$	$\Delta G= 3.49$

Fig. 12. Optimized structures and relative energies for 1-Li-1 without lithium cation solvation (a) and for solvation with one (b), two (c), and three (d) THF molecules ( $\text{kcal mol}^{-1}$ ).

allowance for zero-point vibrations  $\Delta E^0$  as a criterion of the direction of lithiation was chosen. Additional problem arising in calculations is an association of lithium derivatives in solution. Depending on the polarity of solvent PhLi, for example, can exist in solution as dimers, tetramers, hexamers, and (or) even larger associates [34]. Monomers as contact ion pairs (CIP) without Li–C bond cleavage (the formation of solvent-separated ion pairs seems to be improb-

able for these systems) can occur in polar solvents. In these monomers, the lithium cation in most cases is additionally coordinated to several solvent molecules [35]. The lithium derivatives in the solid state are often crystallized as dimers in which the lithium cation is additionally bound by several solvent molecules [36]. However, a dimer formation in polar THF is unlikely for the sterically hindered and electron-deficient lithium derivatives of the

	
1-Li-1 $\Delta E^0=0$	2-Li-1 $\Delta E^0=-0.99$
	
5-Li-1 $\Delta E^0=4.26$	6-Li-1 $\Delta E^0=7.03$
	
1-Li-2 $\Delta E^0=0$	2-Li-2 $\Delta E^0=0.53$
	
3-Li-2 $\Delta E^0=0.52$	6-Li-2 $\Delta E^0=7.18$
	
1-Li-3* $\Delta E^0=0$	2-Li-3 $\Delta E^0=3.09$

**Fig. 13.** Optimized structures and relative energies of lithium salts for **1**, **3**, **5**, and **7** solvated by two THF molecules ( $\text{kcal mol}^{-1}$ ). The structures with lithium localization to the noncoordinated ring for complex **3** were not calculated. For comparison, see Fig. 11.



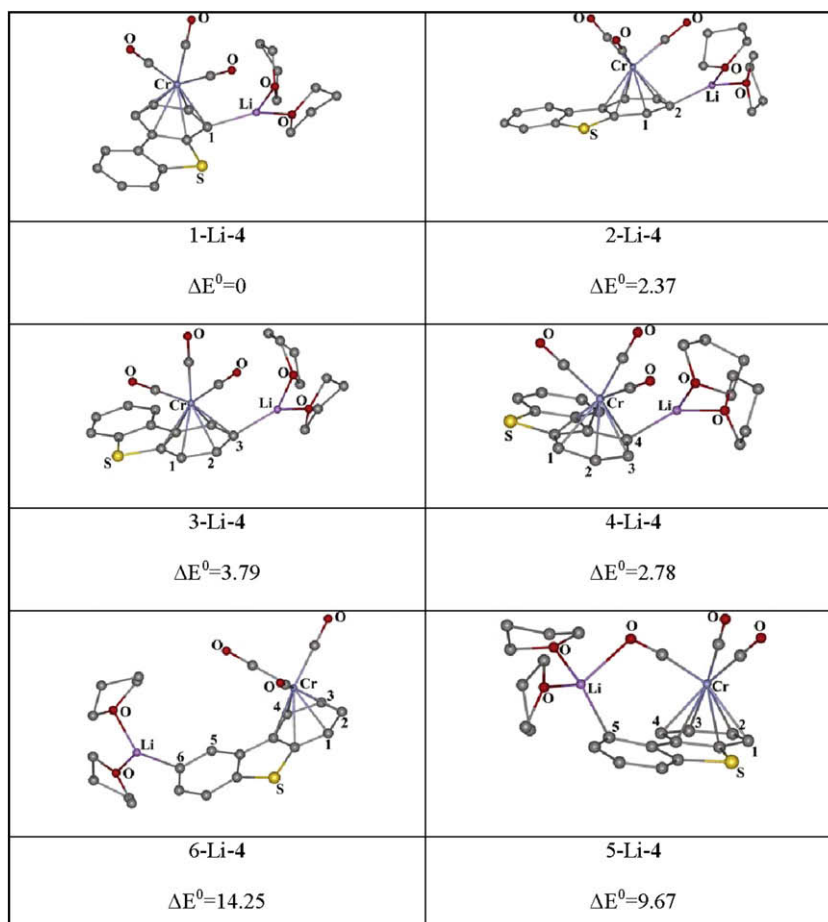


Fig. 13 (continued)

arenetricarbonylchromium complexes due to coordination to the strong acceptor, *viz.*, tricarbonylchromium group. In addition, lithium derivatives without coordination to a transition metal have a covalent Li–C bond [37]. This distinguishes them from ionic compounds, such as fluorenyllithium, capable of forming solvate-separated ion pairs. Taking the aforesaid into account, only monomeric molecules were considered as a model for the theoretical analysis of the lithiated complexes. In these species lithium in contact ion pairs is covalently bonded to one carbon atom and additionally binds several THF molecules. As known [34,35], in the lithium salts of polyaromatic ligands without coordination by a transition metal in both solution (NMR data) and solids (X-ray diffraction data), the lithium atom is often additionally coordinated to solvent molecules (ether, THF) or other coordinating agents (tetramethylethylenediamine, crown ethers, etc.). Therefore, calculations for the lithium salt of the tricarbonylnaphthalenechromium complex 1-Li-1 were performed with one, two, and three THF molecules (THF is a standard solvent used for lithiation) involved in solvation and localized in vicinity of the lithium atom. It follows from these data that when the entropy factor is necessarily taken into account [18,35] by the calculation of the free Gibbs energy, the successive addition of one and then the second THF molecule decreases the free energy of the system  $\Delta G$  for tricarbonylchromium complex 1-Li-1 in THF, while the addition of the third molecule in contrast increases  $\Delta G$ . The results of calculations are given (Fig. 12).

It follows from the results of calculations (Fig. 12) that when the entropy factor is necessarily taken into account [18,35] by the calculation of the free Gibbs energy, the successive addition of one and then the second THF molecule decreases the free energy of

the system  $\Delta G$  for tricarbonylchromium complex 1-Li-1 in THF, while the addition of the third molecule in contrast increases  $\Delta G$ .

Thus, one can conclude that a monomer, in which lithium is covalently bonded to carbon and additionally coordinated by two THF molecules, can be used as a model for quantum chemical analysis of lithiated arenetricarbonylchromium complexes. Note that additional coordination lithium with two solvent molecules eliminates binding of lithium with the carbonyl. Using this model, structures and energies of different possible lithium derivatives of complexes **1**, **2**, **3**, and **4** solvated by two THF molecules were calculated (Fig. 13).

The data in Fig. 13 show that for the lithium derivatives of the tricarbonylchromium complexes of naphthalene **1**, biphenyl **2**, biphenylene **3**, and dibenzothiophene **4**, the DFT method predicts well the regioselectivity of lithiation, *i.e.*, preferential formation of the derivatives in which the lithium atom is localized near the coordinated ring. Note that the difference in energies with allowance for zero-point vibrations  $\Delta E^0$  has been used. For example, lithium derivatives **1**, **2**, **3**, and **4** exhibit a considerable increase in  $\Delta E^0$  (up to 14 kcal mol<sup>-1</sup>) for the lithium binding to the noncoordinated ring as compared to the lithium binding to the ring bound to chromium. This is consistent with the experimental data on the absence of this lithiation direction. For complexes **1** and **2**, lithiation to the coordinated ring of which is not selective, the energy difference is low (for the lithiated complex **2**  $\Delta E^0$  for the *ortho*-, *meta*-, and *para*-isomers of lithium salts 1-Li-2, 2-Li-2, and 3-Li-2 differ less than by 0.58 kcal mol<sup>-1</sup>, whereas for 1-Li-1 and 2-Li-1 they differ by 0.48 kcal mol<sup>-1</sup>). For selectively metallated complexes **3** and **4** the difference is at least 2.37 kcal mol<sup>-1</sup>. For

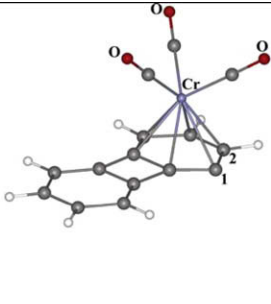
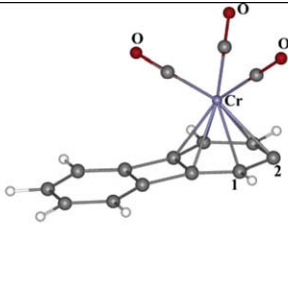
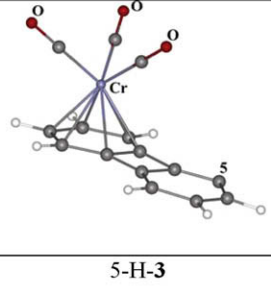
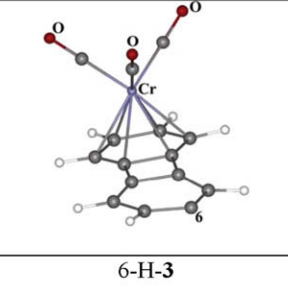
	
1-H-3 $\Delta E^0=0$	2-H-3 $\Delta E^0=3.70$
	
5-H-3 $\Delta E^0=10.95$	6-H-3 $\Delta E^0=15.34$

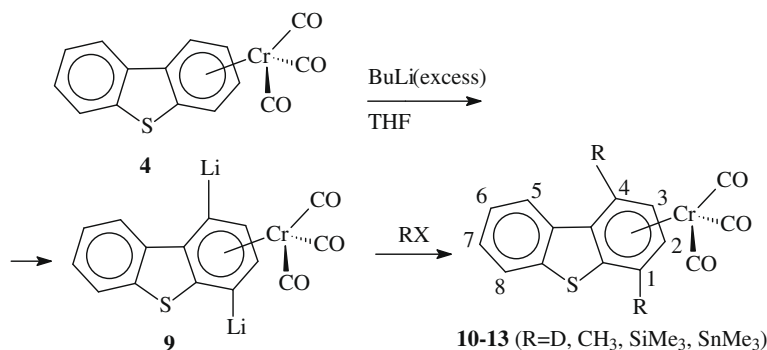
Fig. 14. Optimized structures and relative energies of anions 1-H-3, 2-H-3, 5-H-3, and 6-H-3 in solvent-separated ion pairs of lithium salts **3** (kcal mol<sup>-1</sup>).

**1**, the  $\Delta E^0$  values describe correctly the preferential formation of isomers **1b**. A very small differences in  $\Delta E^0$  for complex **2** do not allow one to predict the ratio of complexes [**2a**]/[**2b**]/[**2c**] substituted to different positions (see Table 13). Interestingly, for 1-lithium derivative **7** the DFT calculation indicates no stabilizing coordinative interaction with the heteroatom (sulfur atom), which was assumed in many works on the metallation of aromatic heterocycles and their tricarbonylchromium complexes.

The formation of solvent-separated ion pairs for lithium derivatives **1**, **2**, **3**, and **4**, in which the lithium cation is separated from the negatively charged ligand and does not covalently interact with this ligand, is highly improbable. The formation of solvent-separated ion pairs is usually typical of salts of aromatic anions, such as cyclopentadienyl, indenyl, and fluorenyl anions, where the ligand is stabilized due to the formation of an aromatic structure. Nevertheless, the DFT calculation of a possibility of formation of these hypothetical anions as solvent-separated ion pairs for anions

1-H-3, 2-H-3, 5-H-3, and 6-H-3 (the first figure means the position in complex **3** from which H<sup>+</sup> was removed) was performed. The data of calculations for the anions are presented (Fig. 14).

It appears from these data that lithiation to the noncoordinated ring is *thermodynamically* unfavorable in spite of the substantially simplified model ofSSIP for lithium salts **3**, because the corresponding anion has a very high energy. The selectivity of lithiation at position 1 is determined by a higher energy of the aromatic anion without proton in position 2. A similar calculation was carried out for complex **4**. In this case, the relative energies  $\Delta E^0$  for positions 1, 2, 3, and 4 in the coordinated ring are 0, 4.14, 6.01, and 0.97 kcal mol<sup>-1</sup>, respectively, while they range from 11.46 to 19.83 kcal mol<sup>-1</sup> for the noncoordinated ring. Thus, the preliminary calculation of the energies of the corresponding hypothetical “free” anions can be considered as a first estimation, which helps one to decrease considerably the time expenses.



Scheme 13.

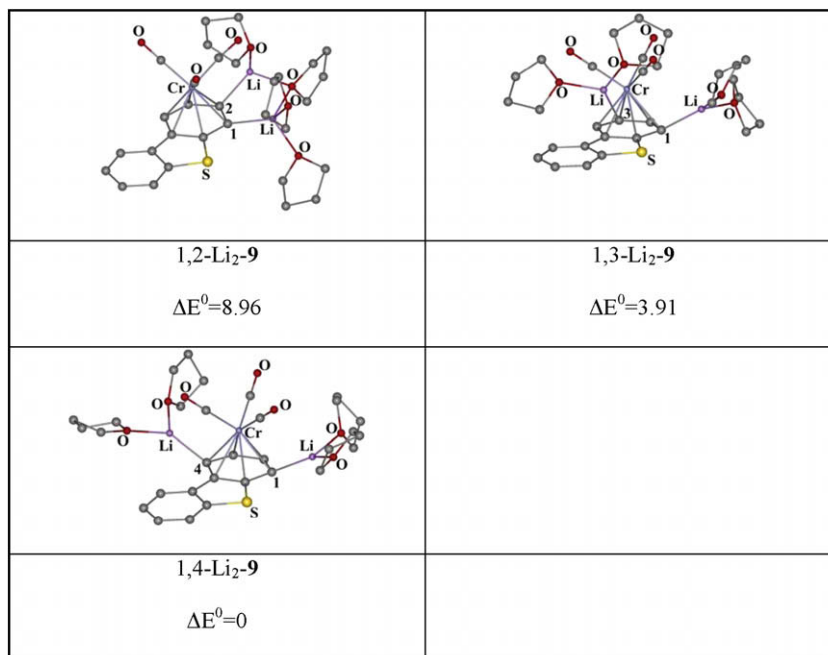


Fig. 15. Optimized structures and relative energies of possible dilithium derivatives **9** for the double metallation of **4** at the coordinated ring (kcal mol<sup>-1</sup>).

It was shown previously [13] than in the excess of BuLi, complex **4** is doubly metallated to form dilithium derivative **9**, the double metallation occurs at positions 1 and 4. This is also supported by the fact that the reaction of dilithium derivative 1,4-Li<sub>2</sub>-**9** with electrophiles RX (R = Me, SiMe<sub>3</sub>, SnMe<sub>3</sub>) affords only 1,4-R<sub>2</sub>-derivatives **10–13** (Scheme 13). The energies of different possible dilithium derivatives Li<sub>2</sub>-**9** were also calculated by DFT (Fig. 15).

As follows from the data (Fig. 15), the energy of derivative 1,4-Li<sub>2</sub>-**9** is minimum and differs considerably from the energies of other possible structures. The result is the formation of 1,4-disubstituted complexes **10–12** (Scheme 13). Double lithiation at the noncoordinated ring was not considered because this reaction should be *a priori* thermodynamically unfavorable.

### 3. Conclusions

As a result of extensive research from the author's laboratory and literature analysis, it was shown that density function theory (DFT) method holds great promise in adequately describing chromium tricarbonyl and other transition metal complexes with any additional coordination sphere. Important parameters, such as structural and conformational peculiarities, different aspects of reactivity, and distinct reaction pathways could be investigated by DFT. Determination of thermodynamic and kinetic parameters for reactivity of transition metal complexes is often complicated by considerable experimental difficulties, especially when dealing with extreme instability and high cost of the substances. DFT thus offers an important alternative for a detailed investigation of dynamic behavior of organometallic complexes, having applications as catalysts, metallodrugs or special materials at low time and material expense. In the case of chromium tricarbonyl complexes with polycyclic aromatic carbo- and heterocyclic ligands (PAL), DFT determines precisely, both in solid state, solution and gas phase, structure and conformation, including such delicate effects as bonds distances and short and long bonds alternations, and predicts adequately barriers of rotation of an organometallic group. It was particularly shown that DFT describes well thermodynamic and kinetic parameters of interring haptotropic rearrangements (IRHR) and theoretically calculates activation

barriers ( $\Delta G$ ,  $\Delta E$  or  $\Delta E^\circ$ ) in the region of 25–35 kcal mol<sup>-1</sup> that correspond well to experimentally measured values. DFT also allows one to follow a detailed mechanism of IRHR which proceeds, in general, via periphery of an aromatic ligand with the reducing of hapticity in the intermediates and transition states and the elongation of Cr–C distances in comparison with the initial complex. This method also describes the reactions of the arenetricarbonylchromium complexes with alkyllithium compounds. As was shown, considering only kinetic factor, which is determined by transition state energy in the course of reaction organolithium compound with chromium complex of PAL, it is possible to illustrate selectivity of metallation in coordinated ring in comparison with noncoordinated, but impossible to explain stereoselectivity of lithium localization in coordinated ring. On contrary, the thermodynamic factor, which depends on the energy  $\Delta E^\circ$  (relative energy with allowance for zero-point vibrations) of solvated contact ion pair of lithium salt of the chromium tricarbonyl–PAL complex, appears to be the main criterion for the direction of lithiation to the coordinated aromatic ring and for the selectivity of C–Li bond formation in this ring. DFT can as well adequately describe double (and in general multiple) lithiation to coordinated ring of transition metal complexes of aromatic ligands, which was demonstrated with the example of dibenzothiophenechromiumtricarbonyl  $\eta^6\text{-C}_{12}\text{H}_8\text{SCr}(\text{CO})_3$ .

### Acknowledgements

The authors are grateful to the Alexander von Humboldt Foundation (Bonn, Germany) for the donation of computer for YFO using which a part of preparatory DFT calculations was done. This work was supported by the Russian Foundation for Basic Research (Grant Nos. 96-03-3241 and 96-03-32733), as well as by INTAS Grant No. 94-2921.

### Appendix A. Supplementary material

Supplementary data associated with this article can be found, in the online version, at doi:10.1016/j.jorganchem.2008.11.067.

## References

- [1] (a) A. Berger, J.P. Djukic, Ch. Michon, *Coord. Chem. Rev.* 225 (2002) 215–238; (b) M.F. Semmelhack, in: E.W. Abel, F.G.A. Stone, G. Wilkinson (Eds.), *Comprehensive Organometallic Chemistry II*, vol. 12, Pergamon Press, Oxford, UK, 1995, p. 1017; (c) P.J. Dickens, J.P. Gilday, J.T. Negri, D.A. Widdowson, *Pure Appl. Chem.* 62 (1990) 575.
- [2] (a) Yu.F. Oprunenko, *Russ. Chem. Rev.* 69 (2000) 683. and references therein; (b) T.A. Albright, P. Hofmann, R. Hoffmann, C.P. Lillya, P.A. Dobosh, *J. Am. Chem. Soc.* 105 (7) (1983) 3396–3411.
- [3] K.M. Nicholas, R.C. Kerber, E.I. Stiefel, *Inorg. Chem.* 10 (7) (1971) 1519–1522.
- [4] C. White, S.J. Thompson, P.M. Maitlis, *J. Chem. Soc., Dalton Trans.* (1977) 1654.
- [5] E.P. Kündig, C. Perret, S. Spichiger, G. Bernardinelli, *J. Organomet. Chem.* 286 (1985) 183.
- [6] R. Benn, R. Mynott, I. Topalovic, F. Scott, *Organometallics* 8 (4) (1989) 2299–2305.
- [7] A. Stanger, *Organometallics* 10 (1991) 2979–2982.
- [8] K.H. Dötz, R. Dietz, *Chem. Ber.* 110 (1977) 1555; K.H. Dötz, H.C. Jahr, *Chem. Rec.* 4 (2) (2004) 61–71; K.H. Dötz, N. Szesni, M. Nieger, K.J. Nattinen, *Organomet. Chem.* 671 (2003) 58–74.
- [9] Yu.F. Oprunenko, N.G. Akhmedov, S.G. Malyugina, V.I. Mstislavsky, V.A. Roznyatovsky, D.N. Laikov, Yu.A. Ustynyuk, N.A. Ustynyuk, *J. Organomet. Chem.* 583 (1–2) (1999) 136–145.
- [10] (a) E.P. Kündig, V. Desorby, C. Grivet, B. Rudolph, S. Spichiger, *Organometallics* 6 (6) (1987) 1173–1180; (b) R.U. Kirss, P.M. Treichel Jr., *J. Am. Chem. Soc.* 108 (1986) 853.
- [11] Yu.F. Oprunenko, I.A. Shaposhnikova, Yu.A. Ustynyuk, *Metalloorg. Khim.* 4 (1993) 684; Yu.F. Oprunenko, I.A. Shaposhnikova, Yu.A. Ustynyuk, *Organomet. Chem. USSR* 4 (1993) (Engl. Transl.).
- [12] Yu. Oprunenko, I. Gloriovzov, K. Lyssenko, S. Malyugina, D. Mityuk, V. Mstislavsky, H. Günther, G. von Firks, M. Ebener, *J. Organomet. Chem.* 656 (2002) 27.
- [13] M.V. Zabalov, I.P. Gloriovzov, Yu.F. Oprunenko, D.A. Lemenovskii, *Izv. Akad. Nauk. Ser. Khim.* 1484 (2003); M.V. Zabalov, I.P. Gloriovzov, Yu. F. Oprunenko, D.A. Lemenovskii, *Russ. Chem. Bull. Int. Ed.* 52 (2003) 1567.
- [14] Yu. Oprunenko, S. Malyugina, A. Vasil'kov, Ch. Elschenbroich, K. Harms, *J. Organomet. Chem.* 641 (2002) 208.
- [15] Yu.F. Oprunenko, S.G. Malyugina, Yu.A. Ustynyuk, N.A. Ustynyuk, D.N. Kravtsov, *J. Organomet. Chem.* 338 (1988) 357–368.
- [16] Yu.F. Oprunenko, S.G. Malyugina, N.A. Ustynyuk, Yu.A. Ustynyuk, *Izv. Akad. Nauk. Ser. Khim.* 2 (1988) 433; Yu.F. Oprunenko, S.G. Malyugina, N.A. Ustynyuk, Yu.A. Ustynyuk, *Russ. Chem. Bull. Int. Ed.* 2 (1988) 442.
- [17] Yu. Oprunenko, S. Malyugina, P. Nesterenko, D. Mityuk, O. Malyshev, *J. Organomet. Chem.* 597 (2000) 42–47.
- [18] N.A. Ustynyuk, B.V. Lokshin, Yu.F. Oprunenko, V.A. Roznyatovsky, Yu.N. Luzikov, Yu.A. Ustynyuk, *J. Organomet. Chem.* 202 (3) (1980) 279–289.
- [19] T. Ziegler, *Chem. Rev.* 91 (1991) 651.
- [20] D. Laikov, *Chem. Phys. Lett.* 281 (1997) 151.
- [21] J.P. Perdew, K. Burke, M. Ernzerhof, *Phys. Rev. Lett.* 77 (1996) 3865.
- [22] Gonzalez, H.B. Schlegel, *J. Phys. Chem.* 94 (1990) 5523.
- [23] F.L. Hirschfeld, *Theoret. Chim. Acta* 44 (1977) 129.
- [24] (a) S. Ketrat, S. Müller, M. Dolg, *J. Phys. Chem. A* 111 (2007) 6094–6102; (b) J.O.C. Jiménez-Halla, J. Robles, M. Solà, *J. Phys. Chem. A* 112 (2008) 1202–1213; (c) S. Brydges, N. Reginato, L.P. Cuffe, C.M. Seward, M.J. McGlinchey, *C.R. Chim.* 8 (2005) 1497–1505; (d) F. Nunzi, F. Mercuri, F. De Angelis, A. Sgamellotti, N. Re, P. Giannozzi, *J. Phys. Chem. B* 108 (2004) 5243–5249; (e) K.H. Dötz, J. Stendel Jr., S. Müller, M. Nieger, S. Ketrat, M. Dolg, *Organometallics* 24 (2005) 3219–3228.
- [25] V. Kunz, W. Nowacki, *Helv. Chim. Acta* 50 (1967) 1052–1056.
- [26] K.W. Egger, *J. Am. Chem. Soc.* 89 (1967) 3688–3691.
- [27] R.F.W. Bader, *Atoms in Molecules: A Quantum Theory*, Oxford University Press, Oxford (UK), 1990.
- [28] A. Berger, J.-P. Djukic, Ch. Michon, *Coord. Chem. Rev.* 225 (2002) 215–238.
- [29] (a) M.F. Semmelhack, J. Bisaha, M. Crazny, *J. Am. Chem. Soc.* 101 (1979) 768; (b) P.D. Woodgate, Y. Singh, C.E.F. Rickard, *J. Organomet. Chem.* 560 (1998) 197; (c) Y. Kondo, J.R. Green, J. Ho, *J. Org. Chem.* 58 (1993) 6182.
- [30] R.J. Card, W.S. Trahanovski, *J. Org. Chem.* 45 (1980) 2555.
- [31] (a) M. Häkansson, C.-H. Ottosson, A. Boman, D. Johnels, *Organometallics* 17 (1998) 1208; (b) J.J. Brooks, W. Rhine, G.D. Stucky, *J. Am. Chem. Soc.* 94 (1972) 7339.
- [32] (a) J. Betz, F. Hampel, W. Bauer, *Org. Lett.* 2 (2000) 3805; (b) J. Betz, W. Bauer, *J. Am. Chem. Soc.* 124 (2002) 8699; (c) J. Betz, F. Hampel, W. Bauer, *J. Chem. Soc., Dalton Trans.* 12 (2001) 1876.
- [33] Yu. F. Oprunenko, *Dr. Sci. (habilitation) Thesis*, Chemistry Department, M.V. Lomonosov Moscow State University, Moscow, 1999.
- [34] W. Bauer, *Lithium Chemistry*, in: A.A.-M. Sapse, Schleyer P.v.R. (Eds.), Wiley-Interscience Publications, New York, 1995.
- [35] J. Smid, in: M. Szwarc (Ed.), *Ions and Ion Pairs in Organic Reactions*, Wiley-Interscience Publications, New York, 1972.
- [36] H. Hope, P.P. Power, *J. Am. Chem. Soc.* 105 (1983) 5320.
- [37] J. Betz, F. Hampel, W. Bauer, *J. Chem. Soc., Dalton Trans.* (2001) 1876.